PCCP

Accepted Manuscript

ROYAL SOCIETY OF CHEMISTRY

www.rsc.org/pccp

Journal Name

ARTICLE

Can silicon substituted metal–free organic dyes achieve better efficiency compared to silicon free organic dyes? A computational study

Received 00th January 20xx,
Accepted 00th January 20xx

DOI: 10.1039/x0xx00000x

www.rsc.org/

Abul Kalam Biswas,[a,b] Amitava Das,[*,c] and Bishwajit Ganguly[*,a,b]

The power conversion efficiency of metal-free organic dyes in dye-sensitized solar cells (DSSCs) is now comparable to the ruthenium-based polypyridyl and zinc-based porphyrin dyes. We have investigated the structural, electronic and optical properties of a series of metal free organic dyes and their corresponding silicon substituted dyes computationally. The DFT and TD-DFT calculations revealed that silicon substituted organic dyes should have higher efficiency than the corresponding silicon free organic dyes. The computational results showed that the presence of silole unit as spacer group can significantly affect the performance of DSSCs compared to the typically used thiophene as spacer unit. These results corroborate the experimental observations reported in the literature. The time-dependent density functional theory (TDDFT) calculations performed with CPCM–CAM–B3LYP/6–31+G* level of theory showed better agreements with the experimental absorption spectra of some reported metal free organic dyes having silole in the spacer group compared to other functionals and employed in this study. Indoline donor based dye **5** showed much shorter absorption spectrum (absorption peak at 425 nm) and smaller electron injection driving force ($\Delta G_{injection} = -1.77$ eV) than the corresponding dye **8** containing silicon substituted indoline as a donor and silole group as a spacer unit. The λ_{max} = 502 nm and $\Delta G_{injection} = -1.82$ eV calculated for dye **8** is much larger than the corresponding silicon free dye **5**. The silicon based dye **8** helps to achieve much lower $\Delta G_{regeneration}$ value than **5**, which can facilitates the faster electron injection rate from dye to the semiconductor TiO_2. Dye **8** also should have higher V_{oc} value compared to other dyes (**5-7**) due to favourable interaction with the electrolyte (I^-/I_3^-). The higher planarity and better conjugation in the dye **8** facilitates the transfer to electron from the dye molecules to the semiconductor TiO_2. The calculations performed with phenyl protecting groups near the silicon center of the dye molecule **8** to diminish the dimerization process showed very similar optical properties as obtained with the corresponding unprotected dye system. The designed julolidine and pyrrolo-indolizine donor based dyes also showed similar trend as observed with Indoline donor based dyes.

1. Introduction:

The design and realizations of metal-free organic sensitizers have been of current interest for their applications in dye sensitized solar cells (DSSCs). The performance and stability of DSSCs have gained great improvements since the pioneering work of O'Regan and Grätzel in 1991.[1] Although, inorganic solar cell still dominates the photovoltaic field, its application in technologies is limited due to higher cost or hazardous materials involved in the process.[2-6] Ruthenium and zinc complexes have been demonstrated as important materials for photovoltaic applications.[8-19] Due to the higher cost, low synthetic yield, tedious synthetic procedures, purification protocols and a resource restriction of the noble metal ruthenium, considerable efforts have been made to the development of metal-free organic sensitizers in recent years.[20-23] The design and synthesis of a large number of metal-free organic dyes have drawn widespread academic and commercial attention mainly because of the abundance of raw materials, low cost, the flexibility of molecular design and the higher molar extinction coefficients. Several organic molecules such as triphenylamine, indoline, coumarin, cyanine, perylene, carbazole *etc* have been used as donor groups in D–π–A metal-free organic dyes.[24-30] The efficiency of a D–π–A system is significantly improved with lowering the $E_{0\text{-}0}$ energy-gap.[31] The $E_{0\text{-}0}$ is the electronic vertical transition energy corresponding to the λ_{max}. Efficient electron injection and dye regeneration which are the important parameters for efficient dyes are influenced by the energy location of ground state oxidation potential ($S^{+/0}$) and excited state oxidation potential ($S^{+/*}$).[32] Thus, the aforesaid parameters are important for the design of efficient organic dyes. A few metal-free organic dyes have shown comparable efficiency to metal-coordinated dyes in DSSCs.[33-35]

Recently, silicon based dyes have shown promise for solar cell due to their ability to tune HOMO-LUMO energy levels and excellent stability.[36] The silole unit in polymers and copolymers has

[a] Computation and Simulation Unit (Analytical Discipline and Centralized Instrument Facility), CSIR–Central Salt and Marine Chemicals Research Institute, Bhavnagar–364002, India. *Email:– ganguly@csmcri.org
[b] Academy of Scientific and Innovative Research, CSIR–Central Salt and Marine Chemicals Research Institute, Bhavnagar, Gujarat–364002, India.
[c] Academy of Scientific and Innovative Research, CSIR–National Chemical Laboratory, Pune–411008, India. a.das@ncl.res.in

† Footnotes relating to the title and/or authors should appear here.
Electronic Supplementary Information (ESI) available: [Optimized molecular structures of dyes **5-16** before and after adsorption in the gas phase]. See DOI: 10.1039/x0xx00000x

been investigated for organic photovoltaics, organic field-effect transistors.[37] However, the silicon based dyes have not been investigated extensively for the design of organic sensitizers for DSSCs applications. In this article, we have examined the effect of silicon substitution on the cell performance of a series of metal-free organic dyes having D–π–A structure. The silicon substituted indoline, julolidine and pyrrolo-indolizine donor based organic dyes (containing silabenzene and silole as spacer groups) have shown the promise to enhance the cell performance than the silicon-free organic dye molecules.

2. Computational details

The overall power conversion efficiency (PCE) of a solar cell can be calculated from equation 1.

$$\mathrm{PCE} = \mathrm{FF}\frac{V_{\mathrm{OC}}\,J_{\mathrm{SC}}}{P_{\mathrm{inc}}} \qquad (1)$$

Here, V_{oc} defined as the open–circuit photovoltage, J_{sc} is the short–circuit current density, FF is the fill factor and P_{inc} is the incident solar power on the cell.

The short-circuit current density, J_{sc} in DSSCs is determined as[38]

$J_{sc}=\int_{\lambda} LHE(\lambda)\Phi_{injec}.\eta_{collect}.d\lambda$ (2)

Where $LHE(\lambda)$ is the light harvesting efficiency and it can be calculated by $LHE = 1–10^{-f}$, f is the oscillator strength. Φ_{injec} is the electron injection efficiency and $\eta_{collect}$ is the charge collection efficiency. Φ_{injec} can be calculated through the driving force $\Delta G_{injection}$ (electrons injecting from the excited states of dye molecules to the semiconductor substrate) and it is the difference between oxidation potential of the excited dye (E^{dye*}), and the reduction potential of the CB of the semiconductor (E_{CB}, –4.00 eV).[39]

$\Delta G_{injection} = E^{dye*} – E_{CB}$ (3)

The excited state oxidation potential (E^{dye*}) was estimated by [40]

$E^{dye*} = E^{dye} – \lambda_{max}$ (4)

Where E^{dye} is the ground state oxidation potential of the dye and λ_{max} is the vertical transition energy corresponding to the maximum absorption. The regeneration efficiency (η_{reg}) of the oxidized dye is associated with the regeneration driving force ($\Delta G_{regeneration}$). The dye regeneration ($\Delta G_{regeneration}$) is determined by the differences between the E_{dye} and the redox potential of I^-/I_3^- electrolyte (−4.58 eV).[41] The J_{sc} value in DSSCs increases with increasing the LHE and $\Delta G_{injection}$. The J_{sc} value also increases with decreasing the $\Delta G_{regeneration}$ value.

The V_{oc} in DSSCs can be described by[38]

$$V_{\mathrm{oc}} = \frac{E_c + \Delta\mathrm{CB}}{q} + \frac{k\mathrm{T}}{q}\ln\left(\frac{n_c}{N_{\mathrm{CB}}}\right) - \frac{E_{\mathrm{redox}}}{q} \qquad (5)$$

Where, q is the unit charge, E_c is the conduction band edge of the semiconductor substrate, kT is the thermal energy, n_c is the number of electron in the conduction band, N_{CB} is the density of accessible states in the conduction band, and E_{redox} is the reduction–oxidation potential of electrolyte. ΔCB is the shift of conduction band when the dyes are on the semiconductor.[42]

Computational details

The ground-state geometries were fully optimized using DFT functional i.e., B3LYP and 6–31G* basis set for C, H, O, N, S atoms whereas, effective core potential (ECP) LANL2DZ basis set for Ti.[43-45] Positive vibrational frequencies confirmed that the optimized structures have the lowest energy. We have optimized the different conformers of the dyes and performed our further calculations with the most stable conformer (Figure S1 and S2, supporting information). Earlier studies proved that this method could provide reasonable geometry with much lesser computational cost which is comparable to the MP2 optimized geometry.[46] The absorption spectra of dyes were obtained by single-point of the optimized ground-state geometries in tetrahydrofuran (THF) at CPCM–CAM–B3LYP/6–31+G* and CPCM–M06-2X/6–31+G* level of theory.[47-49] THF has been used as a solvent in this study because most of the absorption spectra of silole containing dyes are reported in this solvent.[50] Here we have considered 30 lowest singlet-singlet excitations. The oxidation potential of the dyes were calculated at CPCM–B3LYP/UB3LYP/6–311G** level of theory of the neutral and cationic dye. Dipole moment of the TiO_2 bound dyes were calculated at CPCM–B3LYP/6–31G* level of theory. We have calculated the μ_{normal} of the studied dyes adsorbed onto $(TiO_2)_6$ cluster. The semiconductor surface is parallel to the yz plane and the dipole moment of the dyes along the x-axis is considered as μ_{normal}. All the calculations were performed with the Gaussian 09.[51]

3. Results and discussion

To identify a reliable DFT functional to predict the photophysical properties of dyes with silole systems, we have examined D–π–A pattern organic dyes containing dithienosilole unit as a π-spacer unit (Figure 1). The organic dyes 3-(6-(1-(2-(Carbazol-9-yl)-thiophen-5-yl)-ethynyl)-4,4-dioctyl-dithieo[3,2-b:2′,3′-d]silole-2-yl-)-2-cyanoacrylic acid **(CTDTSCA,** dye **1**), 2-Cyano-3-{5′-{2-{4-[N,N-bis(4-(2-ethylhexyloxy)-phenyl)amino]phenyl}-3,4-ethylenedioxythiophene-5-yl}-3,3′-din-hexylsilylene-2,2′-bithiophene-5-yl}acrylic Acid **(C219,** dye **2**), **TP6CADTS** (dye **3**) and **TPCADTS** (dye **4**) have been optimized with B3LYP/6-31G* level of theory and the absorption spectra of these molecules were computed using TDDFT calculations.[50,52] Five different exchange-correlation functions, including four hybrid functionals (B3LYP, HSEPBE, M062X and BHandHLYP) and one long range corrected function (CAM-B3LYP) with 6-31+G* basis set were employed to calculate the vertical transition energies.[45] The experimental maximum absorption wavelength (λ_{max}) of the reported dyes **1-4** (Fig. 1) and the calculated absorption wavelength (λ_{max}) are given in Table 1.[50,52] The calculated results suggest that M062X and CAM-B3LYP showed in general a better agreement with the experimental results compared to other DFT functional employed for these systems. These DFT functionals are reasonable to predict the absorption spectra λ_{max} of these organic dye molecules, however, slightly overestimates the calculated values. We have considered CAM-B3LYP functional to calculate the UV/Vis absorption spectra of the designed dyes in this study as this method has been extensively employed to calculate the vertical transition energies of D–π–A dye molecules.[53] Nonetheless, we have also reported the λ_{max} at M06-2X/6-31+G* level of theory of the designed dyes for reasonable agreement with the experimental results of the reference dye molecules (Table S1, supporting information).

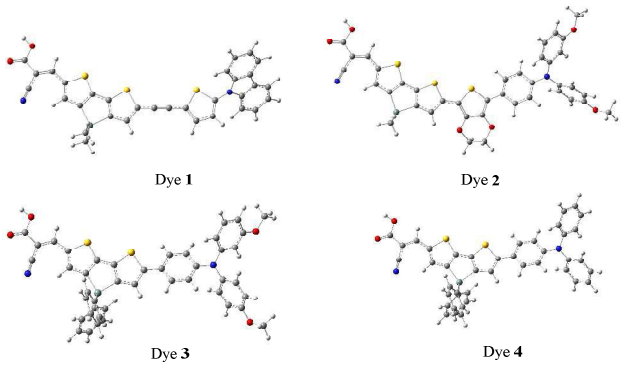

Fig. 1 Optimized geometries of the reported dyes **CTDTSCA** (dye **1**), **C219** (dye **2**) **TP6CADTS** (dye **3**) and

TPCADTS (dye **4**) with silole spacer group.

Table 1. Comparison of experimental and calculated maximum absorption wavelength (λ_{max}) of dyes **1-4**.

Dyes	B3LYP	BHandHLYP	HSEPBE	M06-2X	CAM-B3LYP	Exp[50,52]
1	585	492	595	481	486	450
2	728	549	767	540	540	493
3	668	500	698	496	495	511
4	641	492	666	488	487	495

A few reports with silole unit as a π-spacer in D–π–A dye system has shown promise to enhance the efficiency of DSSCs.[37] The silole spacer unit can possibly help to achieve planarity in D–π–A dye, which subsequently can facilitate the electron transfer to the semiconductor.[37] However, the use of silicon containing dyes have not received much attention despite its improved performance. In this article, we have designed a series of metal-free organic dyes possessing silicon in the donor/spacer units and compared the results with the corresponding silicon free dyes. The silicon free donor groups indoline and julolidines have been considered because of their better efficiency as donor group in organic dyes.[54-61] Pyrrolo-indolizine has been reported however, this group has been exploited as a donor group computationally for the first time.[62] The typical π–spacers fluorenes and thiophene have been chosen and modified in the study.[63-68]

Indoline, julolidine and pyrrolo-indolizine as donor groups with fluorenes and thiophene as π–spacer unit in dye molecules have been examined (dyes **5**, **9** and **13**, Figure 2) computationally. The calculated results of these systems have been treated as reference for the corresponding designed dye molecules containing silabenzene as part of donor groups (dyes **6**, **10** and **14**) and silole spacer groups (dyes **7**, **11** and **15**, Figure 2). Finally the dyes **8**, **12** and **16** (Figure 2) were designed where Si were present in both donor and spacer units. The substitution of thiophene spacer group with silole group is known; however, silicon containing donor group is not reported. The synthesis and isolation of a neutral silaaromatic compound that is stable at ambient temperature was dampened by the high reactivity of Si=C double bonds. However, silabenzene was prepared and found to be stable in THF/Et2O/petroleum ether (4/1/1) solutions at -100°C.[69] Further efforts in this direction led to synthesize and characterize the first neutral silaaromatic species that is stable at ambient temperatures, a 2 silanaphthalene, by taking advantage of an efficient steric protection group, the 2,4,6-tris[bis(trimethylsilyl)methyl] phenyl (Tbt) group.[70] The synthesis of stable 1-Tbt-silabenzene was reported, and its structure was determined by single crystal X-ray structure, which revealed that the silabenzene is planar.[71]

It is well known that in n−type DSSCs, the highest occupied molecular orbital (HOMO) energy level of the dyes should be lower than the redox potential. The value is −4.80 eV in case of I^-/I_3^- redox couple.[72] This ensures avoiding charge recombination between photoinjected electrons in TiO_2 and oxidized dye sensitizers.[73] Moreover, the lowest unoccupied molecular orbital (LUMO) energy level must be above the conduction band of TiO_2 (E_{CB}, –4.00 eV)[39] to inject electrons effectively. The frontier molecular orbital energies of the dyes (**5-8**) are shown in figure 3. The HOMO energy of dye **5** is -6.34 eV, which is below the valance band of TiO_2. The LUMO energy value is -1.92 eV and it ensures the regeneration of the dye. Dye **6** containing silicon substituted indoline as a donor group showed remarkable change in the molecular structure compared to the silicon free dye **5**.

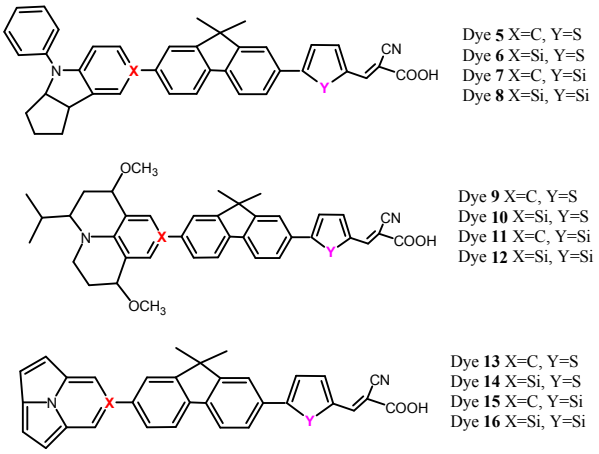

Fig. 2 Molecular structures of the studied dyes **5-16**.

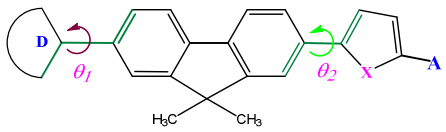

Scheme 1: θ_1 and θ_2 (in green color) are the dihedral angles between the donor and spacer unit as well as the spacer and spacer unit, respectively of D–π–A systems (where D = donor group, X = S or SiH_2 and A = acceptor group).

The longer Si-C bond helps to diminish the steric repulsion between hydrogen atoms of the donor/spacer groups and facilitate attaining planarity (Figure 2). Such changes in the molecular structure of dye **6** resulted in higher conjugation and planarity compared to dye **5**. The planarity is reflected from the dihedral angle (θ) between the donor group and the rest of the dye molecule. The dihedral angle (θ_1) of reference compound **5** is found to be -145.08° which is much smaller compared to **6** (-178.23°) (scheme 1). The conjugation is also reflected from the lower HOMO-LUMO energy gap of dye **6** (3.68 eV) compared to **5** (4.42 eV). In the case of dye **7**, the thiophene group is replaced by silole group and indoline ring has been taken as the donor group (Figure 2). This change in dye **7** reduced the steric repulsion between the hydrogen atom of fluorene and silole that consequently helped to achieve planarity in the system. This arrangement also leads to lower the HLG value (4.18 eV) of **7** compared to **5**. This study has been extended with dye **8**, where the donor and spacer groups contain silicon substituted indoline and silole group, respectively. The HLG value is lowest in the case of **8** (3.43 eV) compared to dyes **5-7**. The geometrical analysis of dye **8** suggests that it achieved better planarity than reference dye **5**. The higher dihedral angles θ_1 (179.51 °) and θ_2 (173.44°) of dye **8** than dye **5** (θ_1 = -145.08° & θ_2 = 156.88°) helps to attain more planarity in

the system. The HOMO-LUMO energies of dyes **5-8** indicated that both the silicon substituted indoline and silole group reduce the HLG but it is lowest for compound **8** which contains silicon containing donor and silole spacer groups. The HOMOs are situated below the redox potential of I^-/I_3^- electrolyte (–4.80 eV) and the LUMOs of all dyes located over the conduction band of the TiO_2 surface (E_{CB}, –4.00 eV) (Figure 3). These favourable energy bands facilitate the electron injection from dye to the TiO_2 surface.

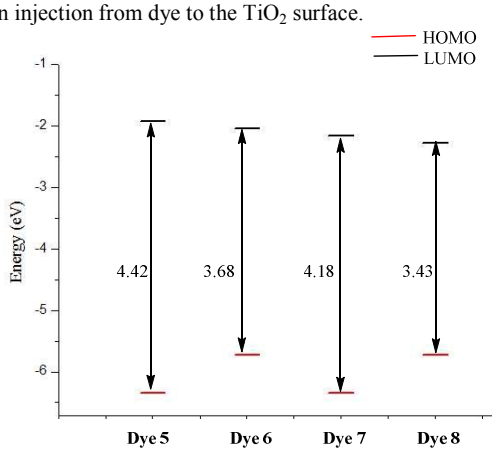

Fig. 3 Frontier molecular energy level diagrams of dyes **5-8**.

We have also examined the influence of silicon substitution on the electronic properties of other studied systems i.e., julolidine based donor dyes **9-12** and pyrrolo-indolizine based dyes **13-16** (Figure 2). Dye **12** containing silabenzene in julolidine as donor group and silole unit in the spacer showed lower HLG than the other dyes (**9-11**) in the series due to higher planarity (Figure S3, supporting information). The larger dihedral angles of dye **12** (θ_1 = -178.23 ° & θ_2 = -171.82°) than the silicon free dye **9** (θ_1 = -144.78 ° & θ_2 = -156.22°) aids to attain higher planarity in the former dye molecule. The pyrrolo-indolizine system has also been explored in dye molecules for DSSCs performance. Similar to **12**, dye **16** with silicon in both donor and spacer groups showed better planarity (θ_1 = -178.47° & θ_2 = -172.18°) than the silicon free dye **13**, which helps for effective conjugation and lower HLG value (Figure S4, supporting information). The calculated results reveal that the presence of Si system in the dye molecules can significantly improve the electronic properties than the corresponding silicon free dyes.

Table 2 Calculated maximum absorption wavelength (λ_{max}/nm, eV), oscillator strengths (*f*), light harvesting efficiency (LHE), and the nature of the transitions for dyes **5–16**.

Dye	State	λ_{max}	Main configuration	*f*	LHE
5	$S_0 \rightarrow S_1$	425 (2.92)	H–1 → L (0.51) H → L (0.41)	1.86	0.986
6	$S_0 \rightarrow S_1$	457 (2.72)	H–1 → L (0.30) H → L (0.55)	1.68	0.979
7	$S_0 \rightarrow S_1$	486 (2.56)	H–1 → L (0.54) H → L(0.40)	1.71	0.981
8	$S_0 \rightarrow S_1$	502 (2.47)	H–1 → L (0.43) H → L (0.51)	1.94	0.989
9	$S_0 \rightarrow S_1$	422 (2.94)	H–1 → L (0.49) H → L (0.46)	1.77	0.983
10	$S_0 \rightarrow S_1$	440 (2.82)	H–1 → L (0.38) H → L (0.51)	1.77	0.983
11	$S_0 \rightarrow S_1$	484 (2.57)	H–1 → L (0.49) H → L (0.47)	1.67	0.979
12	$S_0 \rightarrow S_1$	490 (1.94)	H–1 → L (0.50) H → L (0.49)	1.94	0.989
13	$S_0 \rightarrow S_1$	414 (3.00)	H–1 → L (0.48) H → L (0.46)	1.72	0.981
14	$S_0 \rightarrow S_1$	422 (2.94)	H–1 → L (0.49) H → L (0.42)	1. 90	0.987
15	$S_0 \rightarrow S_1$	473 (2.63)	H–1 → L (0.45) H → L (0.50)	1.60	0.975
16	$S_0 \rightarrow S_1$	475 (2.62)	H–1 → L (0.57) H → L (0.36)	1.80	0.984

The calculated frontier molecular orbitals (FMOs) suggest that in HOMO the orbital contribution is mainly on the donor and the spacer groups and. the LUMO mainly resides on the anchoring and spacer group (Figure S5, supporting information). Such FMOs can show a strong D–π–A character in the molecule which is required for the efficient electron injection from the excited dye to the TiO_2.

The electron injection process from excited dye to TiO_2 can be examined with TDDFT calculations for the studied dyes. These calculations were performed in the CPCM continuum solvation model at CAM-B3LYP/6-31+G* level of theory. The calculated maximum absorption wavelength (λ_{max}), oscillator strength (f) and the corresponding electronic transitions are shown in Table 2 and Figure 4. The absorption wavelength maximum for dye **6** appeared at 457 nm, which is much higher than the silicon free dye **5** (425 nm, Figure 4). The red-shift observed in the case of **6** is due to the lowering of HOMO-LUMO energy gap with the substitution of Si atom in the system (Figure 3). Dye **7** showed even higher absorption maximum (486 nm) than **5** and **6**. Dye **8** showed the highest absorption maximum (502 nm) in the series. Furthermore, we have calculated the absorption spectra of dyes **9-12** and **13-16** (Figure S6, Supporting information). The results followed the similar trend as obtained with **5-8** (Table 2). The calculated results suggest that λ_{max} can be enhanced either by silicon substituted donor group or silole spacer group but the value will be highest for the compound which contains both silicon in donor and spacer group. However, the higher reactivity of Si=C double bonds in silabenzene is known to be a problem.[71] This problem has been circumvented by protecting the silicon center with protecting groups.[71] Hence, we have examined the indoline based dye **8** with phenyl as protecting groups close to the silicon center to avoid the dimerization process (Figure S7, supporting information). The absorption wavelength maximum was found to be 501 nm similar to the unprotected dye **8** (Table S2, supporting information).

DSSCs performance also depends on the short-circuit current density which subsequently depends on the LHE, $\Delta G_{iniection}$ and $\Delta G_{regeneration}$. The LHE, $\Delta G_{iniection}$ and $\Delta G_{regeneration}$ values have been calculated and shown in Table 2 and 3, respectively. The calculated

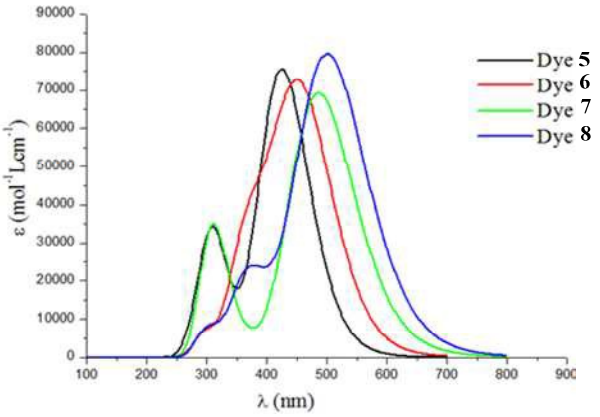

Fig. 4 Absorption spectra of the dyes **5-8** in THF.

results suggest that all the designed dyes **5-8** have very high LHE values and largely comparable. It has been shown that for dye **6**, the $\Delta G_{iniection}$ increases with respect to the reference dye **5** (Table 3). However, the LHE value is slightly lower than dye **5**. Therefore, the J_{sc} of dye **6** may not be very efficient than the dye **5**. The $\Delta G_{iniection}$ and LHE value calculated for **8** is slightly better than the reference dye **5** (Table 2 and 3). The most important changes found for dye **8** compared to dye **5** is $\Delta G_{regeneration}$ value. The $\Delta G_{regeneration}$ value of dye **8** is much lower than dye **5**, which facilitates the faster electron injection rate from dye to TiO_2 (Table 3). The smaller value of dye regeneration also helps to avoid charge recombination between the photooxidized dye and the injected electron and minimize the dye degradation.[74] Therefore, it can be predicted that the dye **8** should have better J_{sc} than the reference dye **5**. The calculated LHE, $\Delta G_{iniection}$ and $\Delta G_{regeneration}$ values for the dyes **9-12** and **13-16**, suggest that dyes containing silicon substituted group as donor and silole as spacer group should have better short-circuit current than the corresponding silicon free systems (Table 2 and 3). The relative trend of $\Delta G_{iniection}$ calculated with **5-8** reveals that the silicon containing donor group (**6**) can improve this parameter compared to the silole spacer unit present in the dye molecule (**7**). The dye **8** with phenyl protecting group also showed much larger $\Delta G_{injection}$ as obtained with **8** (Table S2, supporting information).

Table 3 Calculated E^{dye} (eV), $\Delta G_{injection}$ (eV) and $\Delta G_{regeneration}$ (eV) for dyes **5–16**.

Dye	E^{dye}	$\Delta G_{injection}$	$\Delta G_{regeneration}$
5	5.15	–1.77	–0.57
6	4.66	–2.06	–0.08
7	5.15	–1.41	–0.57
8	4.65	–1.82	–0.07
9	5.34	–1.60	–0.76
10	4.81	–2.01	–0.23
11	5.33	–1.24	–0.75
12	4.81	–1.73	–0.23
13	5.64	–1.36	–1.06
14	5.16	–1.78	–0.58
15	5.61	–1.02	–1.03
16	5.16	–1.46	–0.58

As mentioned in computational methods, μ_{normal} is related to the shift of the conduction band and that will lead to a change in V_{oc}.[75] It has been shown that the larger vertical dipole moment of the adsorbed dye pointing outward the semiconductor surface can yield to larger V_{oc}. The calculated μ_{normal} of the studied dyes are shown in table 4. The calculated results suggest that the dyes containing silicon substituted group as donor and silole as spacer group (dyes **8, 12** and **16**) leads to larger μ_{normal} values than the corresponding silicon free dyes (dyes **5, 9** and **13**) (Table 4 and Figure 5). The dye **8** with phenyl protecting group also showed larger μ_{normal} value than the corresponding dye **5** (Table S2, supporting information).

Table 4 Calculated vertical dipole moment μ_{normal} (units in Debye).

Dyes	μ_{normal}
5	13.58
8	14.22
9	15.69
12	15.98
13	7.77
16	9.43

Journal Name

ARTICLE

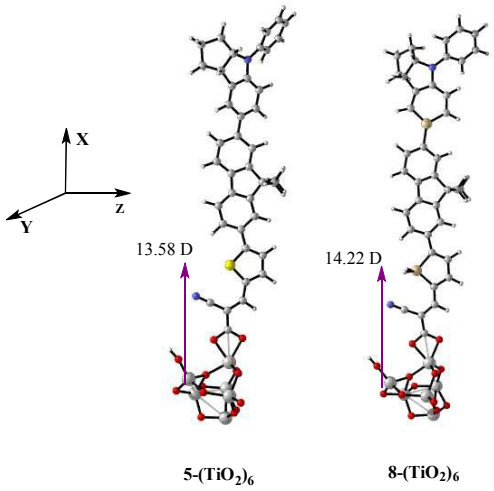

Fig. 5 Calculated vertical dipole moment of dyes **5**-$(TiO_2)_6$ and **8**-$(TiO_2)_6$ at CPCM-B3LYP/6-31G* level of theory in tetrahydrofuran solution. The semiconductor surface is parallel to the yz plane.

The high V_{oc} values also depend on the injected electron in the conduction band of the semiconductor that could recombine with the redox couple (I^-/I_3^-) in the electrolyte and the oxidized organic dyes. It has been perceived that the higher iodine concentration close to the TiO_2 surface, the shorter would be the lifetime in the CB and affect to lower the V_{oc} values.[76,77] We have calculated the dye...I_2 interaction at M06-2X/6-31G* level of theory using LANL2DZ basis set for I atom in the gas phase calculations. It has been reported that the nonbonding interaction of I_2 with CN bond of anchoring group of dye is stronger than I_2...S interaction.[76,77] Thus, we have considered only the I_2...CN interaction in these systems. The optimized molecular structures of the dye...I_2 complexes are shown in figure S8 (supporting information). The CN...I_2 distance for dye **8** (2.814 Å) is longer than the corresponding silicon free dye **5** (2.783 Å). The relatively longer distance of the electrolyte from the anchoring of the dye **8** would help to enhance the electron lifetime in the CB, which subsequently can higher the V_{oc} value compared to the other dye systems studied here. Similar results were also obtained for the julolidine donor based dyes (**9-12**) and pyrrolo-indolizine donor based dyes (**13-16**) (Figure S9, supporting information). The calculated μ_{normal} and I_2...CN interaction distances reveal that silicon substituted dyes should have better V_{oc} compared to silicon free dyes.

Conclusions

In this work, we have performed computational experiments to design a series of metal free organic dyes containing the silicon substituted group as donor and silole group as spacer units to achieve higher efficiency of DSSCs. The silicon substituted dyes modulates the geometry to achieve higher conjugation in the system for better optical properties compared to the silicon free dyes. The level of theory employed in the study has been compared with the known experimental results. The calculated absorption spectra at CAM-B3LYP showed better agreements with the reported experimental absorption spectra of some metal free organic dyes having silole unit in the spacer group. The designed dyes **8**, **12** & **16** with silicon substituted group as donor and silole group in spacer unit showed much redshifted absorption spectra, electron injection driving force, electron regeneration energy and vertical dipole moment compared to their corresponding silicon free dyes **5**, **9** & **13**, respectively. The silicon substituted dye **8** showed the absorption spectrum maximum at 502 nm, whereas the silicon free dye **5** showed the absorption spectrum maximum at λ_{max} = 425 nm. Furthermore, the factors J_{sc} and V_{oc} obtained with silicon substituted dyes help to lower the $\Delta G_{regeneration}$ values responsible for the fast electron injection rate to TiO_2. The dye with protecting groups around the silicon centre shows similar properties obtained with the corresponding unprotected dye system. The enhancement of the optical and electronic properties also observed for silicon based julolidine (**12**) and pyrrolo-indolizine (**16**) dyes as observed with indoline dye **8**. This work is inferred to be useful for designing metal free organic dyes with excellent properties to augment the efficiency of dye-sensitized solar cells. We will explore the importance of N-oxide group in solar dye molecules to augment the efficiency of DSSCs.[78]

Acknowledgements

CSIR-CSMCRI Communication number: 087/2015. Authors thank MSM, DST (New Delhi), SIP, and CSIR (New Delhi), for financial support of this work. AKB is thankful to UGC (New Delhi) for fellowship and AcSIR for enrollment in Ph.D. The authors thankfully acknowledge the computer resources provided by CSIR-NCL, Pune (India). We are also thankful to the reviewers for their suggestions and comments that have helped us to improve the paper.

References

1. B. O'Regan and M. A Grätzel, *Nature,* 1991, **353**, 737−740.
2. A. Hagfeldt, G. Boschloo, L. Sun, L. Kloo and H. Pettersson, *Chem. Rev*., 2010, **110**, 6595–663.
3. X. Kang, J. Zhang, D. O'Neil, A. J. Rojas, W. Chen, P. Szymanski, S. R. Marder and M. A. El-Sayed, *Chem. Mater*., 2014, **26**, 4486−4493.
4. E. Maggio, G. C. Solomon and A. Troisi, *ACS NANO*, 2014, **8**, 409–418.
5. R. Stalder, D. Xie, A. Islam, L. Han, J. R. Reynolds and K. S. Schanze, *ACS Appl. Mater. Interfaces,* 2014, **6**, 8715−8722.
6. J. Yang, P. Ganesan, J. Teuscher, T. Moehl, Y. J. Kim, C. Yi, P. Comte, K. Pei, T. W. Holcombe, M. K.

Nazeeruddin, J. Hua, S. M. Zakeeruddin, H. Tian and M. Grätzel, *J. Am. Chem. Soc.*, 2014, **136**, 5722−5730.
7. W. H. Nguyen, C. D. Bailie, Eva L. Unger and M. D. McGehee, *J. Am. Chem. Soc.*, 2014, **136**, 10996−11001.
8. C. C. Chou, F. C. Hu, K. L. Wu, T. Duan, Y. Chi, S. H. Liu, G. H. Lee and P. T. Chou, *Inorg. Chem*., 2014, **53**, 8593−8599.
9. S. W. Wang, K. L. Wu, E. Ghadiri, M. G. Lobello, S. T. Ho, Y. Chi, J. Moser, F. D. Angelis, M. Grätzel and M. K. Nazeeruddin, *Chem. Sci.*, 2013, **4**, 2423–2433.
10. S. Sinn, B. Schulze, C. Friebe, D. G. Brown, M. Jäger, J. Kübel, B. Dietzek, C. P. Berlinguette and U. S. Schubert, *Inorg. Chem.*, 2014, **53**, 1637−1645.
11. A. El–Shafeil, M. Hussain, A. Islam and L. Han, *Prog. Photovolt. Res. Appl.*, **2014**, *22*, 958–969.
12. H. Ozawa, T. Sugiura, R. Shimizu and H. Arakawa, *Inorg. Chem*., 2014, **53**, 9375−9384.
13. S. Mathew, A. Yella, P. Gao, R. Humphry–Baker, B. F. E. Curchod, N. Ashari–Astani. I. Tavernelli, U. Rothlisberger, M. K. Nazeeruddin and M. Grätzel, *NATURE CHEMISTRY*, 2014, **6**, 242-247
14. L. L. Li and E. W. G. Diau, *Chem. Soc. Rev.*, 2012, **42**, 291-304.
15. J. Luo, M. Xu, R. Li, K. W. Huang, C. Jiang, Q. Qi, W. Zeng, J. Zhang, C. Chi, P. Wang and J. Wu, *J. Am. Chem. Soc.*, 2014, **136**, 265–272.
16. L. Cabau, C. Vijay Kumar, A. Moncho, J. N. Clifford, N. López and E. Palomares, *Energy Environ. Sci*., 2015, **8**, 1368-1375.
17. A. Yella, H-W. Lee, H. N. Tsao, C. Yi, A. K. Chandiran, M. K. Nazeeruddin, E. W-G. Diau, C-Y. Yeh, S. M. Zakeeruddin and M. Grätzel, *SCIENCE*, 2011, **334**, 629-633.
18. M. Urbani, M. Gratzel, M. K. Nazeeruddin and T. Torres, *Chem. Rev*., 2014, **114**, 12330−12396.
19. L-L. Li and E. W-G. Diau, *Chem. Soc. Rev*., 2013, **42**, 291-304.
20. A. Mishra, M. K. R. Fischer and P. Bäuerle, *Angew. Chem., Int. Ed.*, 2009, **48**, 2474–2499.
21. K. Hara, T. Sato, R. Katoh, A. Furube, T. Yoshihara, M. Murai, M. Kurashige, S. Ito, A. Shinpo, S. Suga and H. Arakawa, *Adv. Funct. Mater.*, 2005, **15**, 246–252.
22. C. Teng, X. Yang, C. Yang, S. Li, M. Cheng, A. Hagfeldt and L. Sun, *J. Phys. Chem. C*, 2010, **114**, 9101–9110.
23. S. Ito, H. Miura, S. Uchida, M. Takata, K. Sumioka, P. Liska, P. Comte, P. Pechy and M. Grätzel, *Chem. Commun.*, 2008, 5194–5196.
24. G. Wu, F. Kong, Y. Zhang, X. Zhang, J. Li, W. Chen, W. Liu, Y. Ding, C. Zhang, B. Zhang, J. Yao and S. Dai, *J. Phys. Chem. C*, 2014, **118**, 8756−8765.
25. P. Thongkasee, A. Thangthong, N. Janthasing, T. Sudyoadsuk, S. Namuangruk, T. Keawin, S. Jungsuttiwong and V. Promarak, *ACS Appl. Mater., Interfaces* 2014, **6**, 8212−8222.
26. A. K. Biswas, S. Barik, A. Sen, A. Das and B. Ganguly, J. Phys. Chem. C, 2014, **118**, 20763-71.
27. K. Pei, Y. Wu, A. Islam, S. Zhu, L. Han, Z. Geng and W. *J.* Zhu, *Phys. Chem. C*, 2014, **118***,* 16552−16561.
28. S. Kim, H. Choi, C. Baik, K. Song, S. O. Kang and J. Ko, *Tetrahedron*, 2007, **63**, 11436–11443.
29. H. Choi, C. Baik, S. O. Kang, J. Ko, M. S. Kang, M. K. Nazeeruddin and M. Grätzel, *Angew. Chem. Int. Ed.*, 2008, **47**, 327–330.
30. H. Choi, J. K. Lee, K. Song, S. O. Kang and J. Ko *Tetrahedron*, 2007, **63**, 3115–3121.
31. M. Akhtaruzzaman, A. Islam, F. Yang, N. Asao, E. Kwon, S. P. Singh, L. Han and Y. Yamamoto, *Chem. Commun*., 2011, **47**, 12400.
32. A. Islam, H. Sugihara and H. Arakawa, *J. Photochem. Photobiol., A*, 2003, **158**, 131.
33. Z. Yao, H. Wu, Y. Ren, Y. Guo and P. Wang, *Energy Environ. Sci*., 2015, **8**, 1438-1442.
34. Z. Yao, M. Zhang, H. Wu, L. Yang, R. Li and P. Wang, *J. Am. Chem. Soc*., 2015, **137**, 3799−3802.
35. N. Zhou, K. Prabakaran, B. Lee, S. H. Chang, B. Harutyunyan, P. Guo, M. R. Butler, A. Timalsina, M. J. Bedzyk, M. A. Ratner, S. Vegiraju, S. Yau, C. -J. Wu, R. P. H. Chang, A. Facchetti, M-C. Chen and T. J. Marks, *J. Am. Chem. Soc*., 2015, **137**, 4414−4423
36. (a) C. W. Keyworth, K. L. Chan, J. G. Labram, T. D. Anthopoulos and S. Watkins, *J. Mater. Chem*., 2011, **21**, 11800; (b) G. Lu, H. Usta, C. Risko, L. Wang, A. Facchetti, M. A. Ratner and T. J. Marks, *J. Am. Chem. Soc.*, 2008, **130**, 7670.
37. (a) M. Akhtaruzzaman, Y. Seya, N. Asao, A. Islam, E. Kwon, A. El-Shafei, L. Han and Y. Yamamoto, *J. Mater. Chem*., 2012, **22**, 10771. (b) S. Ko, H. Choi, M-S. Kang, H. Hwang, H. Ji, J. Kim, J. Ko, and Y. Kang, *J. Mater. Chem*., 2010, **22**, 2391.
38. J. Zhang, H. B. Li, S. L. Sun, Y. Geng, Y. Wu and Z. M. Su, *J. Mater. Chem*., 2012, **22**, 568–576.
39. (a) J. Preat, D. Jacquemin, C. Michaux and E. A. Perpète, *Chemical Physics*, 2010, **376**, 56–68. (b) J. Zhang, Y-H. Kan, H-B. Li, Y. Geng, Y. Wu and Z-M. Su, *Dyes and Pigments,* 2012, **95**, 313-321.
40. T. Marinado, K. Nonomura, J. Nissfolk, M. K. Karlsson, D. P. Hagberg, L. Sun, S. Mori and A. Hagfeldt, *Langmuir*, 2009, **26**, 2592–2598.
41. Y. Bai, J. Zhang, D. Zhou, Y. Wang, M. Zhang and P. Wang, *J. Am. Chem. Soc*., 2011, **133**, 11442–11445.
42. S. Rühle, M. Greenshtein, S. G. Chen, A. Merson, H. Pizem, C. S. Sukenik, D. Cahen and A. Zaban, *J. Phys. Chem. B*, 2005, **109**, 18907–18913.
43. A. D. Becke, *J. Chem. Phys*., 1993, **98**, 5648–5653.
44. C. Lee, W. Yang and R. G. Parr, *Phys. Rev. B*, 1988, **37**, 785–789.
45. H-Q. Xia, J. Wang, F-Q. Bai and H-X. Zhang, *Dyes and Pigments*, 2015, **113**, 87-95.
46. J. Preat, C. Michaux, D. Jacquemin and E. A. Perpète, *J. Phys. Chem. C*, 2009, **113**, 16821–16833.
47. S. Karthikeyan and J. Y. Lee, *J. Phys. Chem. A*, 2013, **117**, 10973−10979.
48. (a) M. P. Balanay and D. H. Kim, *Phys. Chem. Chem., Phys*. 2008, **10**, 5121–5127. (b) V. Barone and M. Cossi, *J. Phys. Chem. A,* 1998, **102**, 1995–2001
49. (a) B. Yang, Q. Zhang, J. Zhong, S. Huang and H. Zhang, *Organic Electronics,* 2012, **13**, 2568–2574. (b) S. Kupfer, J. Guthmuller and L. González, *J. Chem. Theory Comput.*, 2013, **9**, 543–554.
50. (a) J. Lui, X. Sun, Z. Li, B. Jin, G. Lai, H. Li, C. Wang, Y. Shen and J. Hua, *Journal of photochemistry and Photobiology A: Chemistry*, 2014, **294**, 54-61. (b) S. Ko, H. Choi, M-S. Kang, H. Hwang, H. Ji, J. Kim, J. Ko, and Y. Kang, *J. Mater. Chem.,* 2010*,* **20***,* 2391–2399.
51. M. J. Frisch, G. W. Trucks, H. B. Schlegel, G. E. Scuseria, M. A. Robb, J. R. Cheeseman, G. Scalmani, V. Barone, B. Mennucci, G. A. Petersson, H. Nakatsuji, M. Caricato, X. Li, H. P. Hratchian, A. F. Izmaylov, J. Bloino, G. Zheng, J. L. Sonnenberg, M. Hada, M. Ehara, K. Toyota, R. Fukuda, J. Hasegawa, M. Ishida,

T. Nakajima, Y. Honda, O. Kitao, H. Nakai, T. Vreven, J. A. Montgomery, Jr., J. E. Peralta, F. Ogliaro, M. Bearpark, J. J. Heyd, E. Brothers, K. N. Kudin, V. N. Staroverov, T. Keith, R. Kobayashi, J. Normand, K. Raghavachari, A. Rendell, J. C. Burant, S. S. Iyengar, J. Tomasi, M. Cossi, N. Rega, J. M. Millam, M. Klene, J. E. Knox, J. B. Cross, V. Bakken, C. Adamo, J. Jaramillo, R. Gomperts, R. E. Stratmann, O. Yazyev, A. J. Austin, R. Cammi, C. Pomelli, J. W. Ochterski, R. L. Martin, K. Morokuma, V. G. Zakrzewski, G. A. Voth, P. Salvador, J. J. Dannenberg, S. Dapprich, A. D. Daniels, O. Farkas, J. B. Foresman, J. V. Ortiz, J. Cioslowski, and D. J. Fox, Gaussian 09, Revision D.01, Gaussian, Inc., Wallingford CT, 2013.

52. (a) L-Y. Lin, C-H. Tsai, K-T. Wong, T-W. Huang, L. Hsieh, S-H. Liu, H-W. Lin, C-C. Wu, S-H. Chou, S-H. Chen and A-I. Tsai, *J. Org. Chem.* 2010, **75**, 4778–4785. (b) W. Zeng, Y. Cao, Y. Bai, Y. Wang, Y. Shi, M. Zhang, F. Wang, C. Pan and P. Wang, *Chem. Mater*., 2010, **22**, 1915–1925.
53. (a) J. Preat, D. Jacquemin, C. Michaux and E. A. Perpete, *Chem. Phys*., 2010, **376**, 56–68. (b) J. Preat, *J. Phys. Chem. C*, 2010, **114**, 16716–16725. (c) M. Pastore, E. Mosconi, F. De Angelis and M. Grätzel, *J. Phys. Chem. C*, 2010, *114*, 7205–7212.
54. H. Choi, J. K. Lee, K. H. Song, K. Song, S. O. Kang and J. Koccc, *Tetrahedron*, 2007, **63**, 1553–1559
55. W. Zhu, Y. Wu, S. Wang, W. Li, X. Li, J. Chen, Z. S. Wang and H. Tian, *Adv. Funct. Mater*., 2011, **21**, 756–763.
56. Y. Z. Wu, X. Zhang, W. Q. Li, Z.-S. Wang, H. Tian and W. H. Zhu, *Adv. Energy Mater*., 2012, **2**, 149–156.
57. Y. Z. Wu, M. Marszalek, S. M. Zakeeruddin, Q. Z. H. Tian, M. Gratzel and W. H. Zhu, *Energy Environ. Sci.,* 2012, **5**, 8261–8272.
58. Y. Cui, Y. Wu, X. Lu, X. Zhang, G. Zhou, F. B. Miapeh, W. Zhu and Z. S. Wang, *Chem. Mater*., 2011, **23**, 4394–4401.
59. Z. Ning, Y. Fu and H. Tian, *Energy Environ. Sci*., 2010, **3**, 1170–1181.
60. W. Q. Li, Y. Z. Wu, Q. Zhang, H. Tian and W. H. Zhu, *ACS Appl. Mater. Interfaces*, 2012, **4**, 1822–1830.
61. S. Y. Qu, C. J. Qin, A. Islam, Y. Z. Wu, W. H. Zhu, J. L. Hua, H. Tian and L. Y. Han, *Chem. Commun*., 2012, **48**, 6972–6974.
62. Y. Tominaga, Y. Shiroshita, T. Kurokawa, H. Gotou, Y. Matsuda and A. Hosumi, *J. Heterocyclic Chem*., 1989, **26**, 477-486.
63. H. Tian, X. Yang, R. Chen, R. Zhang, A. Hagfeldt and L. Sun, *J. Phys. Chem. C*, 2008, **112**, 11023−11033.
64. Z. Peng, S. Tao, X. Zhang, J. Tang, C. S. Lee and S. T. Lee, *J. Phys. Chem. C*, 2008, 112, 2165−2169.
65. A. Baheti, P. Singh, C. P. Lee, K. R. J. Thomas and K. C. Ho, *J. Org. Chem*., 2011, **76**, 4910–4920.
66. M. S. Khan, M. R. A. Al-Mandhary, M. K. Al-Suti, B. Ahrens, M. F. Mahon, L. Male, P. R. Raithby, C. E. Boothby and A. Kohler, *Dalton Trans.*, 2003**,** 74–84.
67. M. Wielopolski, J. Santos, B. M. Illescas, A. Ortiz, B. Insuasty, T. Bauer, T. Clark, D. M. Guldi and N. Martin, *Energy Environ. Sci.*, 2011, **4**, 765–771.
68. D. W. Chang, H. N. Tsao, P. Salvatori, F. D. Angelis, M. Grätzel, S. M. Park, L. Dai, H. J. Lee, J. B. Baek and M. K. Nazeeruddin, *RSC Adv.*, 2012, **2**, 6209–6215.
69. G. Märkl and W. Schlosser, *Angew. Chem., Int. Ed. Engl*. 1988, **27**, 963.
70. N. Tokitoh, K. Wakita, R. Okazaki, S. Nagase, P. v. R. Schleyer and H. Jiao, *J. Am. Chem. Soc*., 1997, **119**, 6951.
71. K. Wakita, N. Tokitoh, R. Okazaki, N. Takagi and S. Nagase, *J. Am. Chem*., Soc., 2000, **122**, 5648-5649.
72. G. Zhang, H. Bala, Y. Cheng, D. Shi, X. Lv, Q. Yu and P. Wang, *Chem. Commun*., 2009, 2198–2200.
73. T. Daeneke, A. J. Mozer, Y. Uemura, S. Makuta, M. Fekete, Y. Tachibana, N. Koumuru, U. Bach and L. Spiccia, *J. Am. Chem. Soc*., 2012, **134**, 16925.
74. M. Li, L. Kou, L. Diao, Q. Zhang, Z. Li, Q. Wu, W. Lu, D. Pan and Z. Wei, *J. Phys. Chem. C*, 2015, **119**, 9782−9790.
75. P. Chen, J. H. Yum, F. D. Angelis, E. Mosconi, S. Fantacci, S. J. Moon, R. H. Baker, J. Ko, M. K. Nazeeruddin and M. Grätzel, *Nano Lett*., 2009, **9**, 2487–2492.
76. W-L. Ding, D-M. Wang, Z-Y. Geng, X-L. Zhao and W-B. Xu, *Dyes and Pigments*, 2013, **98**, 125-135.
77. H-Q. Xia, J. Wang, F-Q. Bai and H-Q. Zhang, *Dyes and Pigments*, 2015, **113**, 87-95.
78. I. Despotović and R. Vianello, *Chem. Commun*., 2014, **50**, 10941-10944.